The Role of Stellar Mass in High-Contrast Imaging

Justin R. Crepp, John A. Johnson

California Institute of Technology

arXiv:1103:4910 (accepted to ApJ)

(a.k.a., a simple explanation of all exoplanet images to date)

(1) Why have the first handful of exoplanet images been around M,K and A stars, but no spectral types in between? This must be telling us something about planet formation.

Star	SpTy	$M_*/M_\odot$	m_p/M_J	V	Assoc.	Age (Myr)	a (AU)	s (pc)	ρ/d
Fomalhaut	A3	2.1	<3	1.2	Castor	200	119	7.7	0.5
β Pic	A6	1.8	8^{+5}_{-2}	3.9	β Pic	10-12	8-15	19.3	0.7
HR 8799	A5	1.6	5-10	6.0	Columba?	20-150	15-68	39.4	1.8
AB Pic	K2	0.8	13.5 ± 0.5	9.2	Tuc-Hor	30	260	47	0.2
GQ Lup	K7	0.7	21.5 ± 20.5	11.4	Lupus	1	103	140	0.2
1RXS J1609	K7	0.7	≈ 8	I=11.0	USco	2-5	330	145	0.1
GSC 06214	M1	0.6	13.5 ± 2.5	I=11.1	USco	2-5	320	145	0.1

Fig. 1: Directly imaged planetary-mass (m<15M_{Jup}) companions with stellar primaries (http://exoplanet.eu/). There currently exists an apparent dichotomy between the detection of planets around A-stars in the solar neighborhood and ultra-wide separation planets around M, K stars in clusters.

(2) The Doppler technique has shown that strong correlations exist between star mass and planet properties:

(1) the occurrence rate of gas giant planets correlates with star mass (Johnson et al. 2010)
(2) planets orbiting A-stars are more massive than those orbiting lower-mass stars (Bowler et al. 2010)
(3) planets orbiting A-stars have wider orbits than those orbiting lower-mass stars (Bowler et al. 2010)

Can extrapolation of the radial velocity (RV) planet population to separations accessible to high-contrast instruments explain the top portion of Table 1? YES!

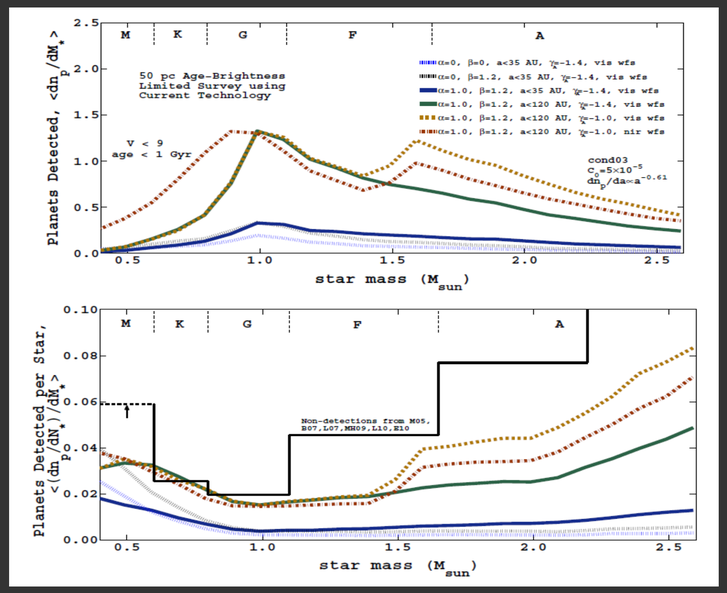

Fig. 2 – Planet detection numbers (top) and rates (bottom) as a function of host star mass for a 50 pc age-and-brightness selected ground-based imaging survey using contrast levels comparable to present-day instruments. Over-plotted are non-detections from a number of previous programs. Extrapolation of the Doppler RV population to wide semimajor axes yields an excellent agreement between simulations and observations to date, in terms of both absolute and relative detection rates. Thus far, only 2 planetary systems have been imaged from the ground in the parameter space considered above (bright, young, nearby stars): HR 8799 and Beta Pic. Both are A-stars. Therefore, the slope of the detection rate curve as a function of star mass must be positive. This occurs when correlations exist between star mass and planet properties.

(3) Two additional observational results support interpretation of Beta Pic b and the HR 8799 planets as forming by "core-accretion":

(i) Beta Pic b and HR 8799 bcde fall in the same sector of the mass / semi-major axis plot as RV planets (Currie et al. 2011).

(ii) Spectra of HR 8799 b indicate a very high metal content (Barman et al. 2011).

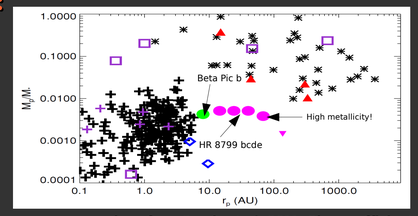

Fig. 3 – Mass ratio vs. semi-major axis for planetary mass companions from Currie et al. 2011. Given sufficient time baselines, Doppler RV teams will eventually discover companions with the same orbital period as Beta Pic b and HR 8799 e (indeed, many RV trends already exist in current data sets!). Given their co-rotation and orbit configuration, it is difficult to justify invoking separate formation mechanisms for HR 8799 e and HR 8799 b. Further, HR 8799 e has a high metal content, and our simulations of an extended (a<100 AU) RV population indicate that it is natural to image the first exoplanets around nearby A-type stars.

(4) How do we explain the bottom portion of Table 1? Observations of a group of stars having the same distance and age represents a special case in high-contrast imaging, neutralizing two important trade-offs between low-mass stars and high-mass stars. Simulations of a tight cluster show that there is a situation where low-mass stars can dominate both the number *AND* efficiency of detections. This occurs when all correlations between star mass and planet properties are removed (the red curves below).

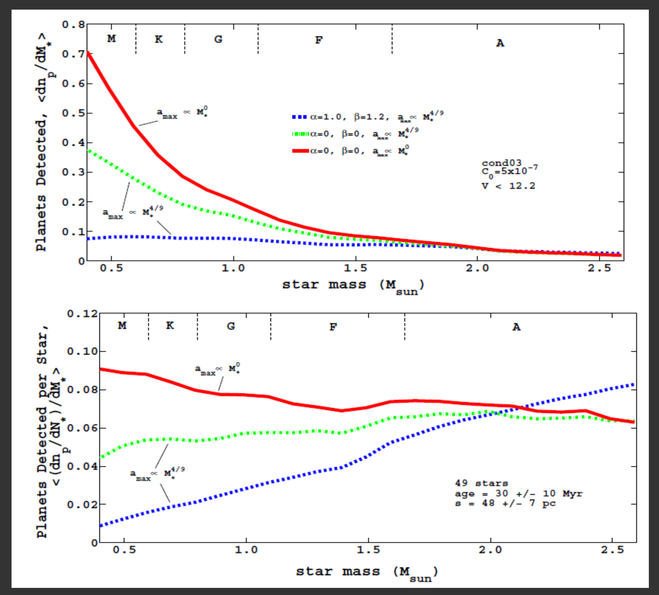

Fig. 4 – Planet detection numbers (top) and rates (bottom) as a function of host star mass for simulations of a young stellar association synthesized to resemble Tucana-Horologium. When correlations between star mass and planet properties are removed, the number of detections essentially follows the IMF.

(5) Table 1 and our simulation results are consistent with the presence of two different planet formation mechanisms: one operating close to stars that results in strong correlations between star mass and planet properties, and another operating further from stars (or possibly at all separations) where there exists little correspondence between star mass and planet properties.

Some observational constraints on the presence of ultra-wide companions:

"Extrapolating the inferred companion mass function to <13M_J, we find that subdeuterium-burning "planetary" companions, if able to form through gravo-turbulent fragmentation, exist in wide orbits around ~1% of Sun-like stars"

Metchev & Hillenbrand 2010

"... naive estimate of the frequency (of ultra-wide planetary-mass companions) is approximately 4% ..."

Ireland et al. 2011

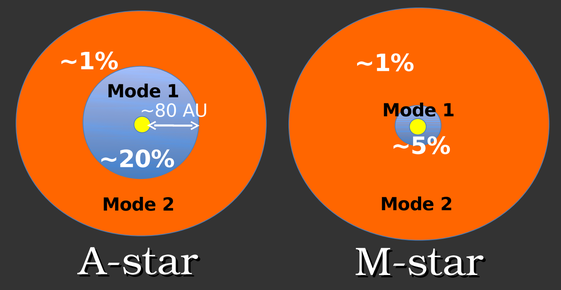

Fig. 5 – The simplest explanation for all exoplanet images to date: two modes of formation. Companions that form close to their star exhibit very strong correlations between star mass and planet properties: planet occurrence rate, semimajor axis extent, and mass all rise with increasing star mass. Mode 1 (blue region) is likely "core-accretion" and is also responsible for creating the Doppler RV planet population. Another mechanism, Mode 2 (orange region) has a lower occurrence rate at wide separations. Our simulations indicate that companions with ultra-wide orbits may exhibit very little correspondence between star mass and planet properties. These results are consistent with the predictions of Boley et al. 2009.

(6) There is another important effect to consider: young stellar clusters are subject to an observational bias related to small number statistics. Low-mass stars produce the first ultra-wide separation exoplanet images irrespective of correlations between star mass and planet properties.

Cluster	N	D (pc)	Age (Myr)
AB Dor	89	34+/-26	70
Argus	64	106+/-51	40
Beta pic	50	31+/-21	10
Tuc-hor	49	48+/-7	30
Columba	41	32+/-30	30
Eta Cha	24	108+/-9	6
Carina	23	85+/-35	30
TW hydra	22	48+/-13	8
Octans	15	141+/-34	20

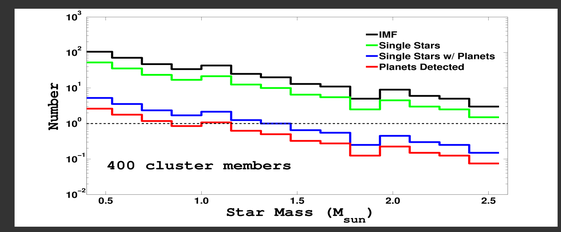

Fig. 6 – The number of detections in a (tightly bound) young stellar cluster always favors low-mass stars. Since the stellar IMF falls off faster than the planet occurrence rate grows, MK stars are the first spectral-types to produce planet images. This bias is exacerbated by the fact that: (i) half of star systems are binaries and high-contrast teams avoid binaries; (ii) the youngest stars are at a distance of ~140 pc, forcing the overall planet occurrence rate to take on its value at wide separations; (iii) the occurrence rate of ultra-wide separation planets appears to be only several percent!

(7) Conclusions:

(i) Extrapolation of the Doppler RV planet population to wide (tens of AU) separations results in an excellent match between simulations and observations to date, both detections and non-detections.

(ii) HR 8799 bcde and Beta Pic b likely formed by the same process as those of the Doppler RV population.

(iii) A-stars are ideal high-contrast imaging targets for reasons in addition to their intrinsic youth and ability to serve as a bright beacon for "extreme" AO systems.

(iv) Observations of a young, tightly bound cluster represents a special case in high-contrast imaging where MK-stars dominate the number of detections.